JOURNAL OF THERMOPHYSICS AND HEAT TRANSFER
Vol. 9, No. 3, July–September 1995

Atomic Species Radiation from Air Modeled with Direct Simulation Monte Carlo Method

M. A. Gallis* and J. K. Harvey†
Imperial College of Science, Technology, and Medicine, London, SW7 2BY England, United Kingdom

This article deals with the evaluation of thermal radiation from atmospheric atomic species with the direct simulation Monte Carlo method under conditions of nonequilibrium. Models to calculate bound-bound, free-bound, and free-free radiation are introduced. This new scheme attempts to improve and extend an earlier approach towards a more detailed modeling of the mechanism of radiation. The results are compared against experimental results and the differences are discussed and evaluated.

I. Introduction

THE shock layer of a re-entry vehicle provokes the development of an extended region in thermal and chemical nonequilibrium in the flow between the vehicle and the shock layer. Due to the high temperatures behind the shock layer, excitation of the internal energy mode takes place that is followed by chemical activity and thermal radiation, the result of electronic excitation. As a result of this chemical activity, high-enthalpy flows have most of their molecular species dissociated to a large degree. In such a flow atomic species are the major source of radiation. It has been found[1] that in some cases the atomic species radiation can contribute up to 80% of the total radiation.

The most effective mechanism for the electronic excitation of the heavy particles is collisions with electrons. Electrons are very effective in transferring their energy to a bound electron of the heavy particle, thereby exciting it to a higher state or even releasing it from the attraction of the nucleus, thus ionizing the particle. This is not the only mechanism though. Electronic excitation is possible even without the presence of electrons. Flows having a lower enthalpy content than that necessary to cause ionization can be electronically excited. Collisions between atoms can be an alternative mechanism, and although this is less effective than the electron–atom collisions in slightly ionized flows, it becomes particularly important since it is the only one. Additionally, secondary radiation mechanisms are associated with the presence of electrons in the flow. These mechanisms are emitting radiation during the neutralization of ions or during the movement of electrons in the electric field of the ions (Bremsstrahlung). These last two mechanisms are not associated with transitions between particular states, and therefore, the energy of the emitted photons is not monochromatic.

Although the electronic excitation of atoms is a mere energy exchange process and the impact of radiation on the flow characteristics is not decisive, there are a number of novel phenomena that are introduced. Absorption of the emitted radiation may lead to further excitation or ionization. Experimental results have shown that electronically excited particles may be effective in promoting reactions in a similar way that vibrational energy controls dissociation reactions. Radiation may also be absorbed by the surface of the vehicle, adding to its thermal load. Radiative heating of the surface usually accounts for a small (but significant) fraction of the total heating of the surface. The calculation of electronic excitation and thermal radiation is particularly important though for the calculation of the emitted signatures that can lead to the detection of the vehicle and the determination of its identity and speed.

The scope of this article to present a new method of calculating the most important radiation mechanisms, applied to the direct simulation Monte Carlo (DSMC) method. The new method is an extension of an earlier method of the same authors and it makes use of both theoretical and experimental data to calculate the excitation probabilities. The previous approach dealt with the cases of molecule–electron and atom–electron interactions only. In this article a new more realistic approach for the electron–atom interaction is proposed and methods for the cases of radiation due to atom–atom collisions (bound-bound), ion–electrons collisions (free-bound), and electron–electric field interaction (free-free) are also included in the model.

The calculation of radiation with any statistical method, such as DSMC, has the obvious disadvantage of dealing with radiation from rare species. The solution to this problem is to increase the number of particle simulators until a sufficiently large sample has been obtained. This will impose an overhead on the calculation. Other methods such as the use of weighting factors can also be used for rare species, but in general, this is a technique that is avoided as it can bring with it further problems. However, this disadvantage of the DSMC method is outweighed by its ability to calculate radiation from flows in a high degree of nonequilibrium, a task that is impossible for most continuum solvers.

II. Electronic Excitation of Atomic Species

Although the collisions between atoms is a less effective mechanism for the electronic excitation of atoms, in cases where the degree of ionization is small it can become as significant as the electron–atom collisions. The excitation of atoms by collisions with other heavy particles provides a mechanism by which flows that have energy content below the ionization threshold become electronically excited and, therefore, radiate.

The two mechanisms for the electronic excitation of atoms (atom–atom and electron–atom) are different in principle. In the case of the electron collisions, the projectile electron passes its energy to the bound electron, exciting it to a higher energy level. The phenomenon, therefore, can be treated as a mere interaction between electrons in the potential field of the nucleus. In the case of the atom–atom collisions the two particles temporarily form a molecule. During this period

Received July 20, 1994; revision received Dec. 8, 1994; accepted for publication Jan. 6, 1995.

*Research Associate, Department of Aeronautics. Member AIAA.
†Professor of Gas Dynamics, Department of Aeronautics. Member AIAA.

energy exchange takes place between the two particles. In such a case there is the possibility that energy from the translational or the internal modes is transferred to one of the electrons of the pseudomolecule. The atoms then separate leaving the electrons in their excited state. The same procedure that applies to the collisions between atoms can be applied to collisions between ions and atoms.

In addition to these mechanisms, electronic excitation may be caused by absorption of light (a mechanism common to molecular species as well). Although this phenomenon is extremely uncommon in rarefied flows, it is particularly efficient in resonantly exciting a particle to the state from which the photon originated.

III. Thermal Radiation and Electronic Excitation in DSMC

The DSMC method developed by Bird[2] is a physical simulation of the Boltzmann equation. The flow is simulated with several thousand particles that move and collide within the computational domain. In the framework of DSMC each physical phenomenon is described with a probability of occurrence. The phenomenon occurs if the probability is greater than a random number selected between 0 and 1. Every time that we have a collision all the possible outcomes are considered and the probability of their occurrence is calculated. The basic characteristic of all DSMC models is their computational efficiency. Since each outcome is considered millions of times, the efficiency of the computational model is particularly important, and one may have to sacrifice physical accuracy for computational efficiency. DSMC is applicable to all density regimes, but it is the rarefied one where it becomes favorable to the continuum Navier–Stokes approaches. The current state of the method involves modeling of the nonequilibrium internal and translational energy exchange, chemical and ionic reactions.

In the context of a DSMC simulation we can determine if electronic excitation will take place during an interaction if we know the probability of an encounter resulting in the excitation. The probability of such an occurrence can be calculated with the aid of electronic excitation cross sections. These cross sections in general depend on the species in question, the available energy, the states between which the transition takes place, and on the energy configuration of the particle (vibrational, rotational, and electronic energy state). The case of an encounter resulting in electronic excitation is treated as a mere case of energy exchange. The comparison of the cross section for a particular transition with the total cross section gives the relative probability of this transition to take place. Whenever an encounter (collision) takes place for which there is a potential for excitation, the cumulative distribution is constructed and the outcome is determined by random selection from this distribution.

There are six main air species (N_2, O_2, NO, N, O, and N_2^+) that can be electronically excited, and therefore, radiate. For the four molecular species Bird[2] has proposed a set with the states that are more likely to be excited. Electronic excitation is considered only for these states because the electronic excitation probability of the other states is significantly lower. A similar group of states for the molecular species has been proposed by Park.[1]

The number of electronic states for the atomic species is very large, and so they have to be grouped into a manageable set. According to Bird,[2] eight main groups of states are considered enough for both atomic oxygen and atomic nitrogen. Park[1] in his model proposed 22 groups of states for nitrogen and 19 for oxygen, which allow a finer resolution of the excitation process and a more detailed modeling of thermal radiation. In this study the grouping proposed by Bird has been adopted.

Attempts to simulate thermal radiation for the rarefied hypersonic regime (e.g., Bird[2]; Carlson and Hassan[3]) have used the assumption of an equilibrium distribution of the electronic states after the collision and of the electron velocity before the collision. However, this assumption is inappropriate in this regime where large areas of significant molecular nonequilibrium are met.

A model to simulate the process of electronic excitation due to electron collisions without the assumption of equilibrium was proposed by Gallis and Harvey.[4] In this approach the excitation probability was calculated with the use of measured and calculated cross sections for each possible transition. In the case of a successful excitation event the energy of the particles was assumed to be the energy of the state that the particle was excited to. This process indicated the need for accurate cross sections that would give a realistic description of the excitation process. This need was particularly important for the case of electron–atom collisions that were calculated using a classical mechanics approach.

In the previous Gallis and Harvey[4] model no attempt was made to deal realistically with the atom–atom collision excitation nor with any of the additional radiation mechanisms. The rectification of the deficiency and the use of more precise cross sections for the electron–atom collisions are the subject of this article.

IV. Electron–Atom Collisions

Due to the grouping of atom electronic states that was done to make the simulation of atomic excitation possible, the states cannot be addressed either with their spectroscopic code or with their quantum numbers. This excludes all direct quantum mechanical approaches that could be used to calculate the interaction. In addition to these models there is a number of phenomenological formulas that have been proposed by Seaton, (in Green),[5] Van Regemorter,[6] and others for the cross sections. In most cases these formulas are in good agreement with the available experimental data. The phenomenological formulas of this type require information about the quantum states between which the excitation takes place (oscillator strength), limiting their applicability to cases where this information is known. The excitation probability of a group of states can be calculated with the excitation formula of Gryzinski,[7] which by using the principles of classical mechanics, requires only the energy of the final state as input. According to this method the excitation is reduced to a coulomb interaction between the bound and the projectile electron. Although the Gryzinski formula is very easy to apply, the fact that is based on classical mechanics for the electronic excitation, a phenomenon clearly quantum mechanical, poses a question mark on the suitability of the theory.

Park has made a collection of experimental and theoretical excitation rates for the atomic species to be used as input data to the NEQAIR code. These rates are considered to comprise the most complete and reliable set of excitation rates for the case of electron–atom collisions. They have been obtained from a large number of both theoretical and experimental studies and cover the transitions to all states of interest from any other state.

In light of the previous analysis for the availability of cross sections, and due to the profound difficulty in deriving the excitation probability, it was considered that a cross section database similar to Park's excitation rate database should be used in preference to Gryzinski's approach used in the earlier study by Gallis and Harvey.[4] The shape of the cross section as a function of the energy is similar for all electron–atom transitions. From a finite value at the threshold the cross section peaks at about 2–3 times the threshold energy and then it starts decaying in an almost exponential manner.

A mathematical function that has been found to describe accurately the cross sections for electron–atom interactions is the Green[7] formula which is given in the form

$$\sigma = c[1 - (1/\varepsilon)]^a(1/\varepsilon)^b \tag{1}$$

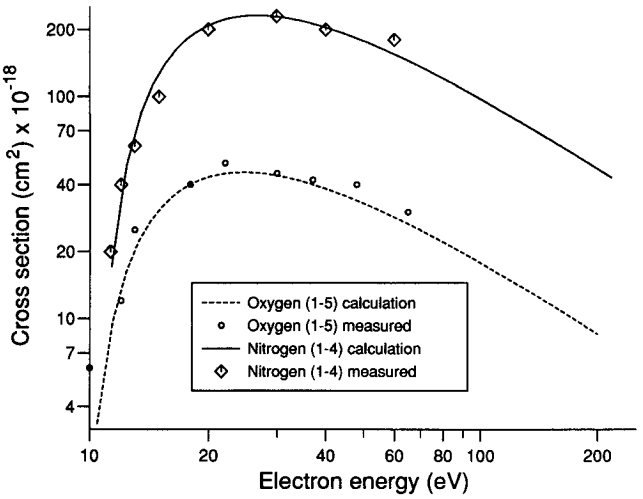

Fig. 1 Electron–atom electronic excitation cross sections.

where ε is the electron energy nondimensionalized by the threshold energy of the transition, and a, b, and c are constant parameters. This formula has been shown to adequately predict the cross section for electron impact excitation for allowed and forbidden transitions for many species. For the application of this formula in the DSMC code the a, b, and c parameters need to be derived. In this study these parameters were calculated so that the resulting excitation rate at equilibrium would match the one given by Park.[1]

The extracted cross sections were compared with experimental data whenever this was possible to verify that the derived cross sections are physically meaningful. Figure 1 shows two examples of cross sections calculated this way, compared with experimentally measured cross sections. The two cross sections correspond to transitions from $2p^4\ ^3P$ to $3s\ ^3S$ (1–5) in atomic oxygen, and from $2p^3\ ^4S$ to $2s\ ^4P$ (1–4) in atomic nitrogen. The experimental results have been taken from Stone and Zipf.[8,9] Similar agreement was achieved for other cross sections where the experimental data were available. From this comparison we conclude that the simulation of cross section with the proposed function can produce results in good agreement with the experimental results. This justifies the use of Eq. (1) for the prediction of the required cross sections.

The constants a, b, and c control different parts of the cross section. In this sense the evaluation of them is possible by matching the corresponding parts of the cross section given in Eq. (1) with the experimental data. The a, b, and c defined this way are not unique, but the comparison with experimental data indicates that the selection of values was successful.

V. Atom–Atom Collisions

The second most important electronic excitation mechanism after the electron–atom collisions is the collisions between atoms. As explained in the Introduction the atom–atom excitation constitutes a completely different excitation mechanism than the electron impact. The latter can even be treated as an interaction between the projectile and the bound electron (coulomb interaction), while atom–atom collisions are interactions between two neutral particles.

The problem of simulating the electronic excitation process due to atom–atom collisions and calculating the electronic excitation probability has so far been treated with simplistic and approximate methods. Park[1] assumed that the electronic excitation rates by atom collisions were a fixed fraction of those of the electron collisions. This fraction was assumed to be 10^{-4}. In a similar manner Bird[2] assumed that the electronic excitation cross sections are a tenth of the equivalent electron–atom ones.

In view of the completely different mechanisms of electronic excitation, the derivation of the atom–atom excitation probability from the electron–atom one can only be considered as approximate and qualitative.

There are a number of quasiclassical and quantum mechanical approaches to calculate the atom–atom cross sections, the description of which is not in the scope of this article. All these methods use information about the interaction potential. The calculation of most of these cross sections requires complicated and time-consuming calculations that prohibit their usage in a DSMC code. For further information the reader should consult Massey[10] or Bates.[11]

In the present analysis we will follow the work of Sobelman and Vainstein[12] to calculate the cross section with an approximate, but fairly accurate, method. The first step is to assume that the interaction potential V can be described with a function of the form

$$V = (\lambda/R^n) - e^{-bR} f(R) \tag{2}$$

where R is the internuclear distance, λ and b are parameters, and $f(R)$ is a polynomial function that satisfies the condition

$$V(R)_{R\to 0} \to \text{const} \tag{3}$$

If we assume that the principal contribution to the transition probability is given for distances $R > 1/b$, this potential function can be further simplified leaving us with a multipole potential function. In this case we can assume a two-state strong coupling approximation. For such a system the cross section for a transition from level i of energy E_i to level f of energy E_f can be calculated approximately as

$$\sigma = 2\pi(\lambda/u)^{2/(n-1)} \exp[-2^{(n+1)/n}\sqrt{\beta_n}\sin(\pi/2n)] I_n(\beta_n) \tag{4}$$

where u is the relative speed of the particles and β_n is a function of the energy difference given as

$$\beta_n = \frac{\lambda^{2/n}[2\pi(E_f - E_i)/h]^{2(n-1)/n}}{u^2} \tag{5}$$

where h is the Planck constant and I_η is given as for $\beta_n \gg 1$:

$$I_\eta(\beta_n) = \tfrac{1}{8}[2\sqrt{2\beta_n}\sin(\pi/2n) + 1] \tag{6}$$

For the case of $\beta_n \to 1$ we have

$$I_2(\beta_2) \to \pi^2/(1/\beta_2)$$

$$I_3(\beta_3) \to \pi/2$$

The order n of the multipole function depends on the type of the interaction and it takes the value of 2 for allowed transitions and 3 for forbidden. For the general case of a collision in which one of the colliding atoms passes from level J_1 to level J_1', and the second one from J_2 to J_2', and both transitions are allowed, the parameter is given as

$$\lambda = \frac{2\pi}{h}\left[\frac{S_{k1}S_{k2}}{g_1 g_2(2n_1 - 1)(2n_2 - 1)}\right]^{1/2} \tag{7}$$

where S_{k1}, S_{k2} are the line strengths of the electric multipole transitions, and g_1, g_2 are the statistical weights of the initial states.

For the case of an allowed transition during an interaction between an ion with atomic number Z and an atom, the previous equation takes the form

$$\lambda = (2\pi/h)Ze(S/3g)^{1/2} \tag{8}$$

This approximate theory describes correctly the transition for the two limiting cases of $\lambda/u \to 0$, $\lambda/u \to \infty$. Examination of

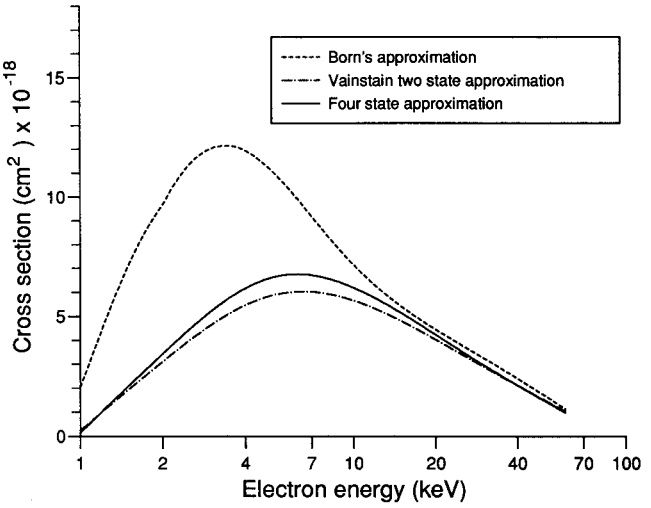

Fig. 2 Atom–atom electronic excitation cross sections for hydrogen.

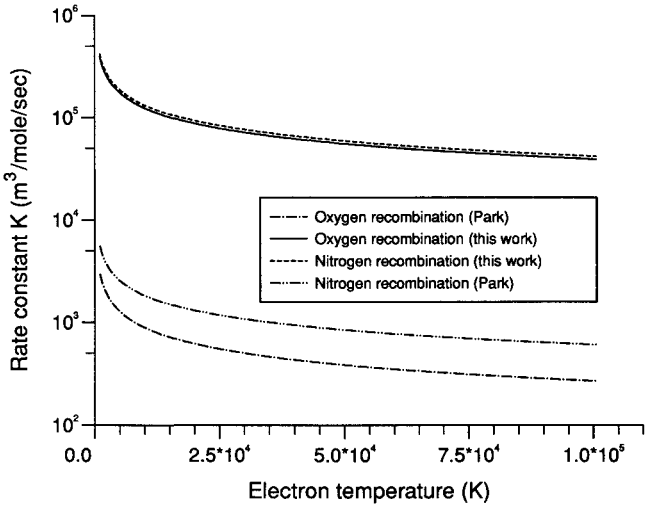

Fig. 3 Comparison of radiative recombination reaction rates.

the special case of transitions in collisions between hydrogen particles where accurate solutions exist shows that this approximation describes fairly accurately the intermediate range as well.

Using this approach the excitation probability for nitrogen and oxygen atoms in the DSMC code was found to be 1–2 orders of magnitude less than the electron–atom one.

Figure 2 (adopted from Massey[9]) shows a comparison of calculations made with Vainstain's method, Born's, and the four-state approximation for the excitation of the 2*s* state of atomic hydrogen. Although the energy range of this figure is well above the energy range of interest in aerospace applications, the example is indicative of the agreement that can be achieved between this method and the more accurate, but also more complicated, and time-consuming four-state approximation. The agreement with the Born cross section is not excellent, but this is expected since the Born cross section becomes reliable only for very high energies.

Simple formulas for the calculation of the cross sections for atom–atom inelastic collisions have been proposed by Landau and Zener and by Demkov (both in Bernstein[13]). According to them the cross section for a collision with energy E can be given as

$$\sigma = \pi R^2[1 - (E_0/E)]G(u/u^*) \tag{9}$$

where R is the radius of the interaction region, E_0 is the mean potential energy in the center of the transition zone, u^* is a parameter with dimensions of velocity, and G is a function of the velocity ratio. It is worth noting that these functions, given appropriate parameters, present similar energy dependence for the cross section as the Vainstain approach.

VI. Continuum Radiation

Radiation can be emitted when a free electron recombines with an ion to form a neutral atom. In the case of aerospace applications the most important neutralization reactions are

$$N^+ + e^- \rightarrow N + h\nu \tag{10a}$$

$$O^+ + e^- \rightarrow O + h\nu \tag{10b}$$

The energy of the emitted photon $h\nu$ can roughly be obtained from the formula

$$\lambda = \frac{hc}{E_{\text{ion}} + E_{\text{elec}} - E_i} \tag{11}$$

where E_{ion} is the ionization potential, E_{elec} is the kinetic energy of the electron, and E_i is the electronic state of the resulting atom. From this equation we conclude that since the electron energy varies from collision to collision, the wavelength of the resulting photon will vary as well. With a continuous distribution of the electron velocity, the wavelength will follow a continuous distribution as well.

The cross section for the absorption of an electron from an ion with atomic number Z to a level n has been given by Zel'dovich and Raizer[14] as

$$\sigma = \frac{128\pi^2 Z^4 e^{10}}{3\sqrt{3} m_e c^3 h^4 u^2 \nu n^3} \tag{12}$$

where ν is the frequency of the emitted photon, c the speed of light, and e and m_e the electron charge and mass, respectively. This formula gives cross sections in the order of 10^{-21} cm^2. Park[15] used Griem's theoretical approach to calculate the radiative recombination rate for oxygen and nitrogen ions. The rates for both reactions as predicted with the two methods are presented in Fig. 3. In both cases (O and N) Park's rate was found to be around two orders of magnitude less than the one given by Zel'dovich's approach, although the shape of both curves are similar.

Zel'dovich and Raizer[14] have calculated the cross section for the reverse phenomenon, i.e., the absorption of a photon by an atom or ion:

$$\sigma = \frac{64\pi^4 Z^4 e^{10} m_e}{3\sqrt{3} c h^6 \nu^3 n^5} \tag{13}$$

In this study the Zel'dovich approach was used. These cross sections can be used to calculate the emission of free-bound and the absorption of bound-free radiation.

Radiation is also emitted from the movement of electrons in the electric field of the ions. Depending on the interaction, electrons may be slowed down giving away part of their energy in the form of photons. The emitted radiation is a function of the electron temperature (electron energy) and the density of charged species in the flow. The emitted radiation can be calculated under the assumption of the Maxwellian distribution of the electron energy.

Finkelnburg and Peters[16] have given the following expression for the total radiant energy emitted per unit volume in the frequency band from ν to $\nu + d\nu$:

$$\varepsilon_\nu = \frac{32\pi^2 Z^2 e^6 N_i N_e}{3\sqrt{3} c^3 (2\pi m_e)^{3/2} (kT_e)^{1/2}} \tag{14}$$

where N_i and N_e are the ion and electron densities, respectively, and T_e is the electron temperature. It is worth noticing that the radiant energy does not depend on the frequency ν.

Since the electron velocities in the flow are 3–4 orders of magnitude greater than the heavy particle velocities, the electron collision frequency is greater than the heavy particle collision frequency. As a result, the electron energy is expected to reach equilibrium quicker than the heavy particles.

VII. Quenching Effects

An excited state can decay either by unimolecular fluorescence or through a bimolecular transfer process. Quenching processes may be divided into chemical quenching (where chemical rearrangement of the species takes place) and physical quenching. The latter can be treated as a special case of inelastic collisions. It would be expected that since the electronic excitation energies are usually quite large (above 1 eV), the conversion to translational or vibrational energy would be difficult. However, experimental results have shown that such processes do occur, and with significant efficiency.[17]

Quenching was considered in this study. In the absence of data describing this process it was assumed that whenever a collision involving electronically excited particles was taking place, the electronically excited particle was losing its energy.

VIII. Computational Results and Comparison with Experiment

A test simulation that has been extensively used as a benchmark case is a shock wave in air at 10.2 km/s, freestream temperature 300 K, and pressure 0.1 torr. These conditions correspond to experiments made originally by Allen[18] and more recently by Sharma.[19]

The first case, at the previous conditions, simulates a shock wave in real air with a binary mixture of nitrogen and oxygen (79% N_2, 21% O_2) at the above conditions. Eleven species chemistry was used and it was found that behind the shock wave almost complete dissociation of the molecular species takes place. Downstream, the degree of ionization was found to be 2.7%. The simulation was performed with 400,000 particle simulators over a computational grid of 1000 cells. Steady state was reached after about 60,000 time steps and sampling started at 70,000. Computations of the same case over a grid of 100 cells with 100,000 particle simulators gave approximately the same results indicating that the presented results are independent of the grid resolution and the number of particles.

The temperature profile of the shock wave is presented in Fig. 4. In this figure the flow comes from the left to the right. At about $x = 0.03$ m the translational energy starts rising and overshoots to about 27,000 K. The rotational temperature follows the translational overshooting to about 20,000 K. The vibrational energy mode that was frozen upstream is activated by the chemical reactions raising the vibrational temperature to about 10,000 K. The electron temperature, i.e., the translational energy of the electrons, overshoots in the area of the shock wave and then quickly equilibrates with the vibrational temperature as predicted by the TTv model of Park.[1] From this figure we notice that nowhere in the shock wave area is equilibrium between any of the energy modes achieved, highlighting the nonequilibrium nature of the phenomena involved. The "near equilibrium" region behind the shock wave corresponds to a flow time of less than 10^{-6} s. The equilibration of the energy modes is not achieved until far further downstream.

Allen's[18] and Sharma's[19] measurements for the spectral radiation from the nonequilibrium region and the near equilibrium region are presented in Figs. 5 and 6, respectively, with solid markers for Sharma's measurements and crosses for Allen's. The results of the previous Gallis and Harvey[4] model are also presented as squares. The new calculation is presented with vertical lines. The experimental results do not agree for all wavelengths, but since Sharma's results are more recent, they are considered to be more reliable. The experimental results by Sharma[19] cover a narrower wave band (0.3–0.7 μ) than Allen's[18] (0.2–1.2 μ).

Close examination of these figures shows that the addition of the atom–atom electronic excitation process enhanced the thermal radiation emitted from the atomic species. A significant shift to higher energies is observed, especially in the nonequilibrium area where most of the atomic lines were previously underestimated. There are two wavelengths, 0.38

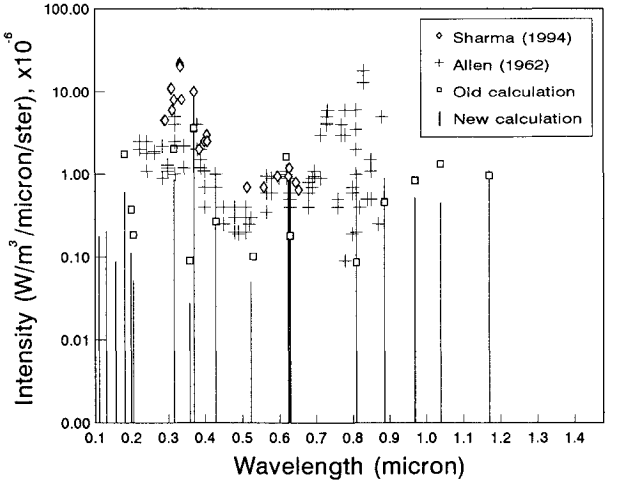

Fig. 5 Air 10 km/s shock wave. Nonequilibrium spectral radiation.

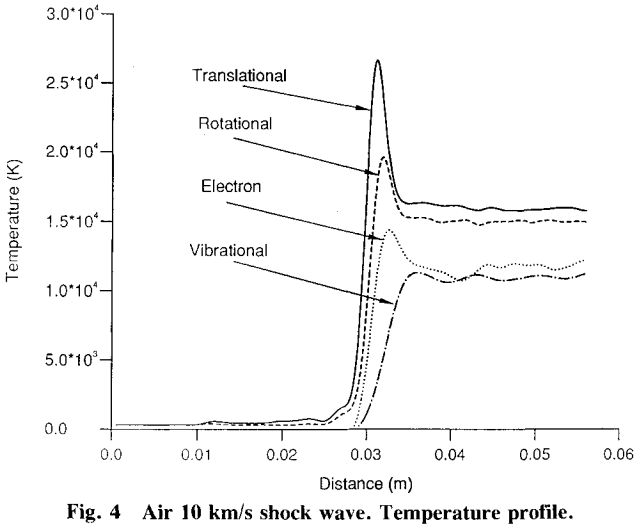

Fig. 4 Air 10 km/s shock wave. Temperature profile.

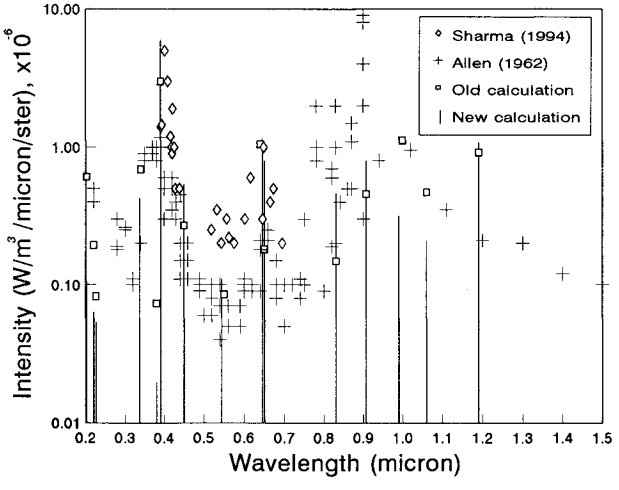

Fig. 6 Air 10 km/s shock wave. Near-equilibrium spectral radiation.

and 0.55, the contribution of which appears to be low. It should be noted that from Sharma's results no line radiation was found to be emitted in these wavelengths. It was only the continuum radiation that was detected. As a result the low contribution of these wavelengths should be expected.

Many of the atomic lines seem to be enhanced, whereas high-energy wavelengths in the region 0.1–0.2 that did not appear with the previous model were accounted for with the new model. This enhanced radiation must be attributed mainly to the added atom–atom excitation mechanism, and secondly to the new electron–atom cross sections. The new excitation model for the atomic species influenced the radiation emitted from the molecular species since a different fraction of the electron energy was made available to them. As a result the radiation from high-energy wavelengths of 0.2 was reduced while the relatively less energetic 0.39 wavelength was enhanced.

The comparison between the experimental results and the DSMC predictions revealed that there are a number of weaker atomic radiation lines that have not been included in this simulation and that will have to be added in future work. By adding these lines the total radiation energy will not change, only its distribution among the lines will change.

The addition of a new electronic excitation mechanism was reflected on the total available energy for radiation. The radiation peak was found to be at 27 MW/m^3 (Fig. 7) compared with 20 MW/m^3 for the previous Gallis and Harvey model. The total radiation emission from the shock wave was not measured in the experiment, but qualitative measurements of the total emitted radiation were obtained from both experiments. These measurements show that the radiation peaks in the nonequilibrium region and then it drops exponentially. From tables,[20] giving the absolute intensity of radiation at various altitudes and velocities, we read that the level of radiation behind the shock for the conditions of the experiment should be 10 W/cm^3. From the measurements presented (Allen and Sharma) we conclude that the nonequilibrium radiation peak should be around 2 to 3 times the value of the equilibrium value, which is in agreement with the prediction above.

Although some discrepancies still exist in the spectral intensity distribution for both the equilibrium and nonequilibrium region, the total radiation seems to be in better agreement with the available data, both qualitatively and quantitatively.

Due to the small concentration of atomic ions (0.5%) the free-bound radiation was found to be too weak in this case. The free-free radiation was calculated and it was found to be two orders of magnitude smaller than the bound-bound radiation.

As a second test case, the rarefied flow around a 70-deg spherically blunted cone was selected. Such flows have recently attracted much interest[21,22] and they have been extensively studied. The flow around a blunted vehicle presents the very interesting feature of areas with very high and very low density. From previous studies it was found that the density of the flow in front of the body is about 120 times the freestream density, and behind the body in the area of the wake the density drops to about 0.1 times the freestream density. This density variation in the same flowfield allows the full band of the radiation mechanisms to be activated with varying significance in different parts of the flow.

The particular test case studied here simulated the flowfield around a 2-m-diam vehicle at 10 km/s at an altitude of 85 km. For the simulation 500,000 particles were used over a grid of 12,330 cells. The calculation took 10,000 CPU minutes on a HP-9000/730 workstation.

The temperature contours as calculated with the new radiation method are presented in Fig. 8. The temperature in this figure has been nondimensionalized with the freestream temperature (185 K) and is presented in Fig. 8. It has been found from previous studies that radiation in most cases does not influence the temperature profiles significantly. Figure 8 can be expected therefore to describe the temperature profiles for both radiation models. The peak average temperature in front of the body was found to be 200 times the freestream temperature (200 × 185 = 36,000 K). Due to the expansion in the wake area the temperature of the high-temperature layer that is formed in front of the body drops to 10 times the freestream temperature. In the wake area and due to a diffuse recompression wave at around $x = 3$ m, the temperature starts rising again in a narrow cylindrical region around the axis of symmetry. The temperature there reaches a value of about 25 times the freestream temperature.

In Figs. 9 and 10 the predictions for the total radiation in W/m^3 are presented with the new and the old model, respectively. From the comparison of these two figures we note that the radiation in front of the body, where all three radiation mechanisms contribute, was enhanced with the new model. The new radiation model predicted a radiation peak of about 0.1 MW/m^3, whereas with the old one the radiation peak was found to be 0.09 MW/m^3. More important differences are found at the back of the body, where the old scheme predicted very weak radiation around the axis of symmetry in the area of the recompression wave. The new scheme predicts a significantly higher radiation activity both around the axis of symmetry and higher in the region between $y = 0.4$ m and $y = 2$ m. The radiation around the axis of symmetry is mostly

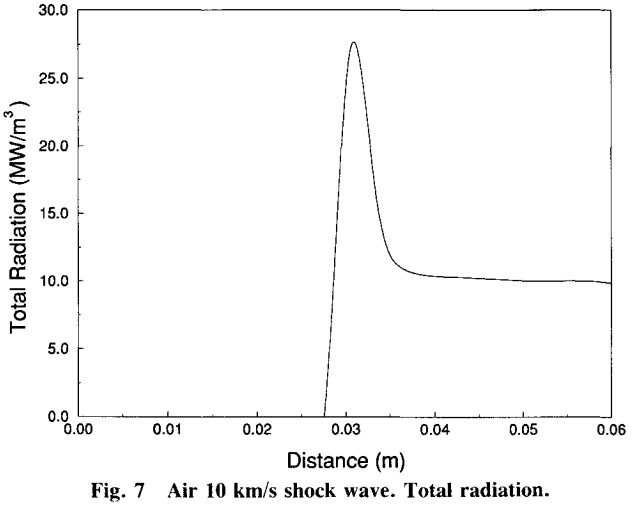

Fig. 7 Air 10 km/s shock wave. Total radiation.

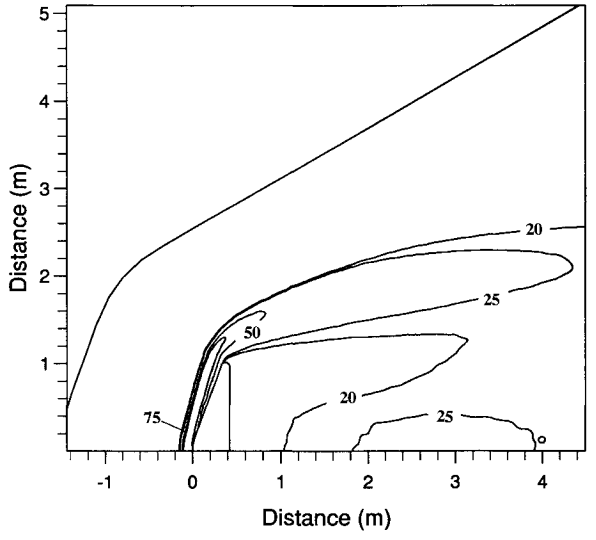

Fig. 8 Cone at 10 km/s. Temperature profile.

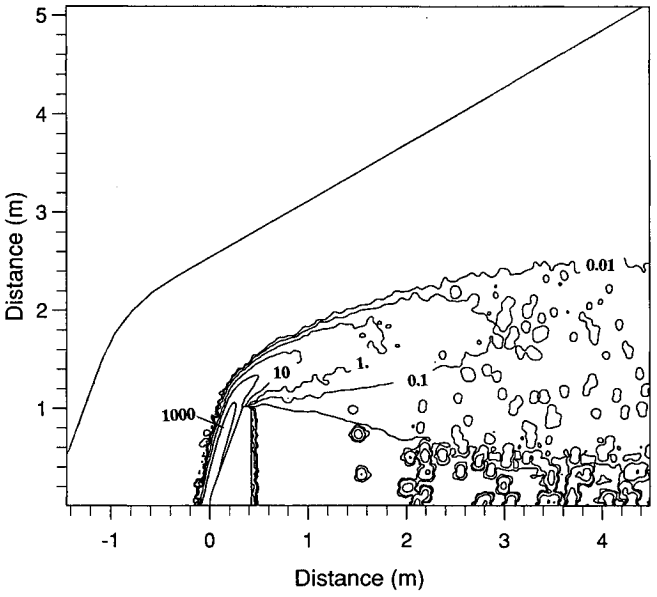

Fig. 9 Cone at 10 km/s. Total radiation with the new model.

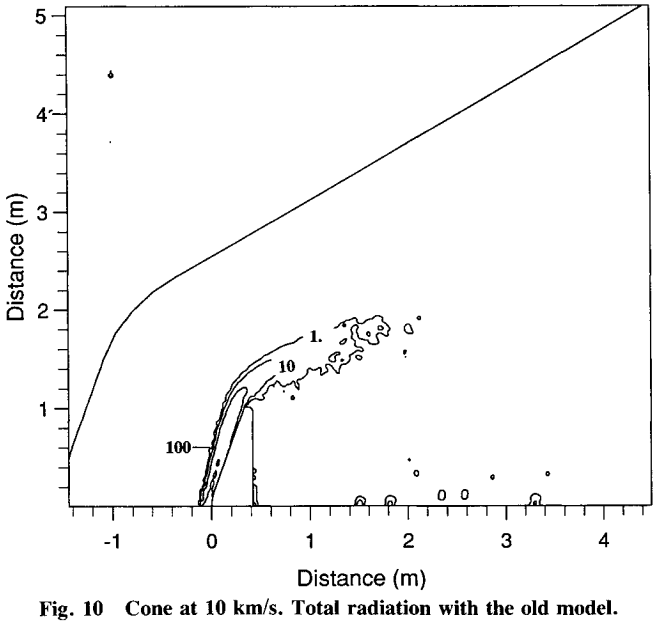

Fig. 10 Cone at 10 km/s. Total radiation with the old model.

due to bound-bound transitions. Bound-bound transitions (atom–atom and electron–atom) are possible in that region because of the local temperature rise (5500 K). The bound-bound radiation emitted from the wake area was found to be atomic, low-energy radiation (large wavelengths). Continuum radiation appears to be the most prominent characteristic of the new radiation profile. This radiation is mostly due to free-free radiation, following the concentration of electrons in the wake, but free-bound radiation was also observed in the form of separated radiation "bubbles" in the "main stream radiation." Statistical noise is inevitable in this case due to the relatively small proportion of particle simulators that radiate. Smoothing of the results has not been applied.

Comparison of the spectral radiation profiles in Fig. 11 shows how the atomic lines are enhanced. In this figure the predictions of the new model are presented with vertical lines, whereas the predictions of the old one are presented with solid squares. In comparison with the old scheme the new one predicts new lines added and the existing ones enhanced. It is important to notice that the new model in both the one-dimensional and the two-dimensional case predicts radiation from the small atomic wavelengths (high-energy photons) in

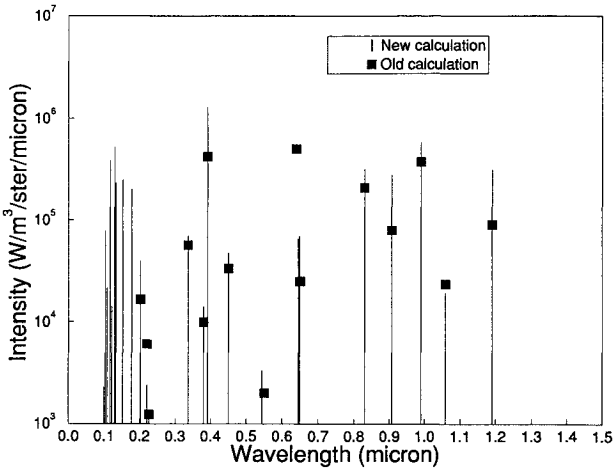

Fig. 11 Cone at 10 km/s. Spectral radiation.

contrast with the previous model. Unfortunately, no validation of these calculations can be done because no spectral data have been published, and they are included only as a demonstration of the ability of the new model.

IX. Conclusions

Simulations of the atomic thermal radiation under conditions of nonequilibrium have been made. To do so available measured and calculated cross sections were used. A model for the calculation of the atom-atom cross sections was developed that allows a fairly accurate and computational efficient simulation of the physical process. For the calculation of the electron–atom cross sections, Park's data were used. Models calculating the continuum radiation were also incorporated into the code.

Improvement was observed in most of the simulated wavelengths. The use of Park's cross sections is considered to be an improvement compared with the Gryzinski formula. It is not easy to quantify this improvement because the uncertainty of these cross sections can be high. It is believed that even if some of these cross sections are in error, no common tendency could force the results in one or the other direction.

Application of the new scheme to low-energy wake flows demonstrated the ability of the method to predict the signatures of flows below the ionization threshold. It was shown that when the electron-impact excitation becomes ineffective, atom–atom collisions and continuum radiation become the main radiation mechanism.

The comparison with the experimental results indicated that there is a number of radiative transitions for atoms that appeared to contribute significantly in the spectral radiation and that have not been included in the present model. The enhancement of the resolution of the radiation model will be the aim of future work.

Acknowledgment

This work was supported by the British Ministry of Defence (D.R.A. Farnborough) under agreement AT/2037/331.

References

[1]Park, C., *Nonequilibrium Hypersonic Aerothermodynamics*, Wiley, New York, 1990.

[2]Bird, G. A., "Non-Equilibrium Radiation During Re-Entry at 10 km/s," AIAA Paper 87-1543, June 1987.

[3]Carlson, A. B., and Hassan, H. A., "Radiation Modelling with Direct Simulation Monte Carlo," AIAA Paper 91-1409, June 1991.

[4]Gallis, M. A., and Harvey, J. K., "Nonequilibrium Thermal Radiation from Air Shock Layers Modeled with the Direct Simulation Monte Carlo," *Journal of Thermophysics and Heat Transfer*, Vol. 8, No. 4, 1994, pp. 765–772.

[5]Green, A. E. S., *The Middle Ultraviolet: Its Science and Tech-*

nology, Wiley, New York, 1969.

[6]Van Regemorter, H., "Rate of Collisional Excitation in Stellar Atmospheres," *Astrophysical Journal*, Vol. 136, 1962, pp. 906–915.

[7]Gryzinski, M., "Two Particle Collisions. II. Coulomb Collisions in the Laboratory Frame of Reference," *Physical Review*, Vol. 138, No. 2A, 1965, pp. 322–335.

[8]Stone, E. J., and Zipf, E. C., "Excitation of Atomic Nitrogen by Electron Impact," *Journal of Chemical Physics*, Vol. 58, No. 10, 1973, pp. 4278–4284.

[9]Stone, E. J., and Zipf, E. C., "Electron-Impact Excitation of the 3S and 5S States of Atomic Oxygen," *Journal of Chemical Physics*, Vol. 60, No. 11, 1974, pp. 4237–4243.

[10]Massey, H. S. W., *Electronic and Ionic Impact Phenomena*, Oxford Univ. Press, Oxford, England, UK, 1971.

[11]Bates, D. R., *Atomic and Molecular Processes*, Academic, London, 1962.

[12]Sobelman, I. I., Vainstein, L. A., and Yokov, E. A., *Excitation of Atoms and Broadening of Spectral Lines*, Springer–Verlag, Berlin, 1981.

[13]Bernstein, R. B., *Atom-Molecule Collision Theory*, Plenum, New York, 1979.

[14]Zel'dovich, Ya. B., and Raizer Yu. P., *Physics of Shock Waves and High Temperature Phenomena*, Academic, London, 1966.

[15]Park, C., "Review of Chemical-Kinetic Problems of Future NASA Missions, I: Earth Entries," *Journal of Thermophysics and Heat Transfer*, Vol. 7, No. 3, 1993, pp. 385–398.

[16]Finkelnburg, W., and Peters, T., *Handbuch der Physik*, edited by S. Fluegge, Vol. 28, 1957.

[17]Levine, R. D., and Bernstein, R. B., *Molecular Reaction Dynamics and Chemical Reactivity*, Oxford Univ. Press, Oxford, England, UK, 1987.

[18]Allen, R. A., Rose, P. H., and Camm, J. C., "Nonequilibrium and Equilibrium Radiation at Super Satellite Re-Entry Velocities," Avco Everett Research Lab., Research Rept. 156, Alexandria, VA, Sept. 1962.

[19]Sharma, S. P., and Whiting, E. E., "Modelling of Non-Equilibrium Radiation Phenomena: An Assessment," AIAA Paper 94-0253, Jan. 1994.

[20]Camm, J. C., Kivel, B, Taylor, R. L., and Teare, J. D., "Absolute Intensity of Non-Equilibrium Radiation in Air and Stagnation Heating at High Altitudes," Avco Everett Research Lab., Research Rept. 93, Alexandria, VA, July 1962.

[21]Dogra, V., Wilmoth, R., Moss, J., Taylor, J., and Hassan, H. A., "Effect of Chemistry and Rarefaction on Blunt Body Wake Structure," AIAA Paper 94-0352, Jan. 1994.

[22]Gallis, M. A., and Harvey, J. K., "Simulation of the Flowfield Around Generic ASTV Configuration Including the Wake," AIAA Paper 94-0353, Jan. 1994.